Vol. 11(1): 136-162, January 2023 DOI: https://doi.org/10.23960/jsl.v11i1.647

P-ISSN: 2339-0913
E-ISSN: 2549-5747

Jurnal Sylva Lestari

Journal homepage: https://sylvalestari.fp.unila.ac.id

Full Length Research Article

Influence of Puspa Wood and Coconut Trunk Combination on the Characteristics of Cross-Laminated Timber Bonded with Polyurethane Adhesive

Siti Aisyah[1], Yusuf Sudo Hadi[1,*], Muhammad Adly Rahandi Lubis[2,**], Muhammad Iqbal Maulana[2], Rita Kartika Sari[1], Wahyu Hidayat[3]

[1] Department of Forest Products, Faculty of Forestry and Environment, IPB University. Jl. Ulin, Kampus IPB Darmaga Bogor, 16680, Bogor, Indonesia
[2] Research Center for Biomass and Bioproducts, National Research and Innovation Agency (BRIN). Jl. Raya Jakarta-Bogor Km. 46, Cibinong, Bogor, 16911, Indonesia
[3] Department of Forestry, Faculty of Agriculture, University of Lampung. Jl. Sumantri Brojonegoro 1, Bandar Lampung, 35145, Indonesia
[*] Corresponding Author. E-mail address: yshadi@indo.net.id
[**]Corresponding Author. E-mail address: marl@biomaterial.lipi.go.id

ARTICLE HISTORY:
Received: 9 September 2022
Peer review completed: 22 September 2022
Received in revised form: 28 December 2022
Accepted: 29 January 2023

KEYWORDS:
Coconut trunk
Cross-laminated timber
Layer combination
Polyurethane adhesive
Puspa wood

ABSTRACT

The purpose of this study was to evaluate the characteristic of cross-laminated timber (CLT) made from puspa (*Schima wallichii*) wood, coconut (*Cocos nucifera*) trunk, and their combination using a polyurethane (PU) adhesive. The manufacturing of CLT begins with the characterization of the adhesive and wood materials used in this study. The CLT panels are made with dimensions of 100 cm × 30 cm × 3.6 cm. The laminate was organized into three layers with the face/core/back, namely puspa wood (PPP), coconut trunk (CCC), and their combination (PCP and CPC), perpendicular to each other using polyurethane adhesive with a glue spread of 160 g.m^{-2}. The physical and mechanical properties of the CLT were assessed according to the JAS 3079 (2019) standard. The results showed that the polyurethane adhesive used in this study could cure optimally at a temperature of 30°C for 200 minutes. Puspa wood and coconut trunk had different physical and chemical properties but had similar wettability to polyurethane adhesives. The physical and mechanical characteristics of coconut CLT were better than puspa CLT. Based on the overall test results, the puspa hybrid CLT is better than the single wood species of the CLT. In contrast to coconut hybrid CLT, the single CLT of CCC was better than its hybrid CLT.

1. Introduction

Wood engineering technology is growing along with the green building movement. Cross-laminated timber (CLT) is a composite product made from laminated oriented perpendicular to each other between layers (Karacabeyli and Douglas 2013). Globally, CLT production in 2019 reached 1.44 million m^3. In 2020 it increased to 2.8 million m^3; by 2025 it is projected to double (UNECE/FAO 2020).

The selection of appropriate raw materials is the basis for determining the quality of CLT. According to ANSI (2018), several wood species are permitted to be used in one CLT panel if the

wood has the same mechanical properties and has a specific gravity of more than 3.5, like softwood. Softwood has a homogeneous structure, so most CLTs are produced using softwood (Aicher et al. 2016; Marko et al. 2016; Wang et al. 2017; Zhou et al. 2020). The production of CLT from softwood has limited raw materials, thus large quantities of raw materials are needed (Mallo and Espinoza 2014). The utilization of hardwood can be an alternative for the production of CLT due to an adequate and sustainable supply of raw materials. In addition, the specific gravity of hardwood is relatively higher than softwood. However, information on tropical hardwood use for CLT production is still limited. Based on this, it is essential to investigate the utilization of hardwood for manufacturing CLT.

One species of hardwood that is commonly found in West Java and can be used as CLT is puspa wood (*Schima wallichii*). Puspa wood has a specific gravity ranging from 0.57 to 0.61 (Hadjib et al. 2010) and meets the requirements of raw materials for CLT, which is 0.35 (ANSI 2018). Characteristics of CLT can be improved by combining it with other wood species. Hybrid CLT has better properties than single CLT (Aicher et al. 2016; Corpataux et al. 2020). One species of wood that can be combined with puspa wood is the coconut trunk (*Cocos nucifera*). Coconut trunks can be used as a material for the production of CLT. Srivaro et al. (2020) reported that the density of coconut trunks ranging from 0.25–0.95 g.cm^{-3} met the raw materials requirement for CLT.

Besides the selection of wood materials, the adhesive used influences the characteristics of the CLT produced. One of the adhesive types that can be used for CLT products is polyurethane adhesive (Karacabeyli and Douglas 2013; Aristri et al. 2021). Several studies on CLT bonded by polyurethane adhesives have been carried out (Hindman and Bouldin 2015; Li 2017; Liao et al. 2017; Wiesner et al. 2021). The CLT products bonded by polyurethane adhesives have better quality than CLTs bonded by other synthetic adhesives (Lu et al. 2018; Hariz et al. 2023; Sikora et al. 2016). The quality of the adhesive in CLT can be influenced by the characteristics of the wood used. Various raw materials have different wood characteristics (anatomical, chemical, and physical properties), so it will affect the characteristics of the CLT (Hovanec 2015; Yusoh et al. 2021). Based on this, it is essential to research the influence of wood species on the CLT characteristics bonded by polyurethane adhesive.

2. Materials and Methods

2.1. Characteristics of Polyurethane Adhesive (PU)

PU adhesive was prepared with an isocyanate: polyol ratio of 1.5:1 (Kong et al. 2011). The solid content of isocyanate was 99.47%, and polyol was 86.73%. The PU adhesive is then tested for its characteristics based on several parameters described below.

2.1.1. Solids Content

The sample of as much as 1 gram of aluminum foil (*Alumunium-foil*, Klinpak, Indonesia) was then put into the oven (Memmert celcius 10.0, Memmert, Germany) at a temperature of 103 ± 2°C for 3 h so that the solution contained in the adhesive evaporates completely. The aluminum foil is removed and then put into a desiccator and weighed. The solid content (SC) value was determined utilizing the following formula:

$$SC\ (\%) = \frac{W1 - Wa}{W0 - Wa} \times 100\% \quad (1)$$

where *W1* is the weight of aluminum foil containing the sample after kiln-dried (g), *Wa* is the weight of empty aluminum foil (g), and *W0* is the initial weight of aluminum foil containing sample (g).

2.1.2. Gelation time

The sample was inserted into the tube case. The measurement of gelation time was carried out using a gel time meter (Techne GT-6, Coleparmer, USA) in position so that the needle was submerged in the sample. Furthermore, the time required for the adhesive to gelatinate was observed at 25°C. The adhesive gelatinization timeout is obtained during the auto-stop time.

2.1.3. Viscosity

The samples used included isocyanates, polyols, and PU with 20 mL each. The samples were placed in a special measuring cup (C-CC27, AntonPaar, Austria) and on a rotational rheometer (RheolabQC, AntonPaar, Austria). Viscosity measurements were carried out with spindle CC no. 27 with rotational speeds of 50/s, 100/s, and 150/s at 25°C to determine the average viscosity. Viscosity results are displayed with the RheoCompass application (AntonPaar, Austria).

2.1.4. Analysis of functional group-FTIR

Functional group analysis was performed using FTIR (FTIR SpectrumTwo, PerkinElmer, United States of America) under liquid and hardened adhesive conditions. Samples of isocyanate, polyols, and polyurethanes were placed and pressed in the holder. The functional group was identified by recording an average of 16 scans at a resolution of 4 cm^{-1} within the wavelength range of 400-4000 cm^{-1}. The curve formation was carried out using the Universal Attenuated Total Reflectance (UATR) method. The resulting spectral pattern is displayed using the origin application (OriginLab, USA), which is then identified for each wave crest.

2.1.5. Analysis of Pyrolysis-Gas Chromatography Mass Spectroscopy (Py-GCMS)

The analysis Py-GCMS was carried out using GC/MS system QP-2020 NX (Shimadzu, Japan) instrument. The sample, as much as 5 g, was put into an eco-cup and then was pyrolyzed at 500°C for 0.1 min using EGA/PY-3030D multi-shot pyrolysis. The pyrolyzed used pressure at 20.0 kPa with 15.9 $ml.min^{-1}$ total flow and 0.61 $ml.min^{-1}$ column flow in helium as carrier gas. The temperature was maintained at 50°C for 1 minute and then increased to 300°C with a heating rate of 10°C.$minute^{-1}$. The result of the Py-GCMS analysis was identified using the NIST LIBRARY 2017 program (NIST MS Search 2.3, Adaptas Solution, USA).

2.1.6. Dynamic Mechanical Analysis (DMA)

The sample was smeared on filter paper (CAT No.1005-125, Whatman, England) according to the glue spread. Then, the filter paper was air-dried. The thermo-mechanical property of adhesive was measured using a DMA instrument (DMA 8000, PerkinElmer, USA) with dual cantilever mode at a constant recurrence pull of 1 Hz at the temperature range of 25-60°C. The

thermo-mechanical response is expressed by storage modulus (E′), loss modulus (E′′), and tan delta by heating each sample at a heating rate of 2°C per minute. Isothermal analysis was performed at 25°C for 200 minutes.

2.2. Characteristics of Material for CLT

2.2.1. Physical and chemical properties

The wood material used in this study was a thirty-year-old puspa (*Schima wallichii*) wood from Gunung Walat Educational Forests, IPB University Forest, and thirty-year-old coconut (*Cocos nucifera*) trunk from Bogor, West Java. The testing of the physical properties of puspa wood and coconut trunk refers to the ASTM D-143:2014 (ASTM 2014) standard. The parameters tested in the physical properties are density, moisture content, and volume shrinkage. In contrast, the testing of chemical properties of puspa wood and coconut trunk included extractive content and pH refers to TAPPI (1991) standard.

2.2.2. Surface roughness

The surface roughness testing refers to the ISO 4287:1997 standard (ISO 1997) with a measured path length of 6 mm, a measuring speed of 0.5 mm per second, and a cut-off of 0.8 mm. Measurements were done following the direction perpendicular to the grain and carried out at five points on the sample surface. The surface roughness measurement parameter used is arithmetical mean roughness (Ra).

2.2.3. Wettability

The wettability measure used the parameter of the contact point between the adhesive and wood surface using the sessile drop method with three replications. The test sample is put on a level table and lined up with the camera. The video results were recorded using the GOM player application in multiples of 10 seconds. The contact angle of each image piece was measured using the ImageJ application with a drop snake plugin analysis. Constant contact angle values were set between time (t) and contact angle (θ) using SAS (Version 9.0, SAS Institute, USA). The *K* parameter value was resolved in view of the S/G model (Shi and Gardner 2001) using the XLSTAT program (Addinsoft Inc., United States of America). The S/G model used the formula:

$$\theta\,(\%) = \frac{\theta i.\,\theta e}{\theta i + (\theta e - \theta i)exp[K(\theta e/(\theta e - \theta i))t]} \quad (2)$$

where θi is the underlying contact angle, θe is the equilibrium contact angle, t is time, and K is the rate of wettability.

2.3. Manufacturing of CLT

The panel was made with a dimension of 100 cm × 30 cm × 3.6 cm (length × width × thickness). Laminates that have been dried and sorted are then arranged. Lamina was organized into three layers with a face/core/back puspa wood (PPP), coconut trunk (CCC), puspa-coconut-puspa (PCP), and coconut-puspa-coconut (CPC), perpendicular to each other using polyurethane adhesive with a glue spread of 160 g.m^{-2}. Then, the CLT panel was cold-pressing with a specific pressure of 0.8 MPa at a temperature of 30°C for 200 minutes (Liao et al. 2017). Then, the CLT panel was conditioned for 7 days to release residual stress due to pressing.

2.4. Physical and Mechanical Properties Testing of CLT

The testing of physical and mechanical properties refers to JAS 3079:2019 (JAS 2019). The sample patterns for cutting the CLT panel test and the dimensions of the sample in this study are shown in **Fig. 1.**

Fig. 1. Test sample cutting pattern. (A= test sample of density, moisture content, and volume shrinkage (3.6 × 7.5 × 7.5) cm^3, B = test sample of water delamination, WA, and TS (3.6 × 7.5 × 7.5) cm^3, C= test sample of boiling delamination (3.6 × 7.5 × 7.5) cm^3, D= test sample backup (3.6 × 7.5 × 7.5) cm^3, E= test sample of MOE and MOR (3.6 × 30.0 × 85.0) cm^3, F= test sample of block shear parallel to the grain (3.6 × 2.0 ×5.0) cm^3, G= test sample of block shear perpendicular to the grain (3.6 × 4.0 × 5.0) cm^3.

2.4.1. Density

The test sample A was measured to the volume (*Va*) and weight (*Wa*) in an air-dried condition. The density (*D*) value was determined utilizing the following formula:

$$D\ (g.cm^{-3}) = \frac{Wa}{Va} \quad (3)$$

2.4.2. Moisture content

The test sample A was measured to the weight (*Wa*) in an air-dried condition. They were kiln-dried at 103 ± 3°C for 24 h and measured the weight again (Wd). The moisture content (*MC*) value was determined utilizing the following formula:

$$MC\ (\%) = \frac{Wa - Wd}{Wd} \times 100\% \quad (4)$$

2.4.3. Volume shrinkage

The test sample A was measured to the volume (*Va*) in an air-dried condition. They were kiln-dried at 103 ± 3°C for 24 h and measured the volume again (Vd). The volume shrinkage (*VS*) value was determined utilizing the following formula:

$$VS\ (\%) = \frac{Vd - Va}{Va} \times 100\% \quad (5)$$

2.4.4. Water absorption

The test sample B was measured to the weight (*W1*) in an air-dried condition. They were immersed at room temperature for 24 h. The weight (*W2*) was measured again after immersion. The water absorption (*WA*) value was determined using Equation 6.

$$WA\ (\%) = \frac{W2 - W1}{W1} \times 100\% \quad (6)$$

2.4.5. Thickness swelling

The test sample B was measured to the average thickness swelling (*T1*) in an air-dried condition. They were immersed at room temperature for 24 h. The average thickness (*T2*) was measured again after immersion. The thickness swelling (*TS*) value was determined utilizing the following formula:

$$TS\ (\%) = \frac{T2 - T1}{T1} \times 100\% \quad (7)$$

2.4.6. Delamination

The test samples B and C were measured to the bond lines on each side and then added up (Σ bond line length). The delamination test was carried out in two tests, namely water and boiling delamination. The water delamination test was conducted by immersing the samples in cold water at 25°C for 24 h and then drained at 70 ± 3°C for 24 h. The boiling delamination test was conducted by soaking in hot water for 4 h and then immersing in cold water for 1 h. After that, samples were oven-dried at 70 ± 3°C for 24 h. The bond lines of the peeling adhesive line on all sides were measured and added up (Σ of the delamination line). Each delamination method was calculated by delamination ratio.

$$Delamination\ (\%) = \frac{\Sigma\ delamination\ length\ (cm)}{\Sigma\ bone\ line\ length\ (cm)} \times 100\% \quad (8)$$

2.4.7. Modulus of elasticity

The test sample E was loaded using Universal Testing Machine (UTM, Baldwin, USA) with a span length of 76 cm and a load speed is 14.7 MPa per minute until the sample broke. The modulus of elasticity (*MOE*) and modulus of rupture (*MOR*) value was determined utilizing the following formula:

$$MOE\ (MPa) = \frac{\Delta PL^3}{4\Delta ybh^3} \quad (9)$$

$$MOR\ (MPa) = \frac{3PL}{2bh^2} \quad (10)$$

where ΔP is the difference between the upper and lower load in proportion limit (N), P is the maximum load (N), L is the span (mm), Δy is the difference of deflection from the top and bottom load (mm), b is the width of sample (mm), and h is the thickness of the sample (mm).

2.4.8. Block shear

The test samples F and G were loaded using UTM Shimadzu (AG-IS 50kN, Shimadzu, Japan) with a load speed of 2 mm/min for parallel to grain and 1 mm/min for perpendicular to the grain. The shear strength value and percentage of wood failure were determined utilizing the following formula:

$$IB\ (MPa) = \frac{Pmax}{A} \quad (11)$$

$$Percentage\ of\ wood\ failure\ (\%) = \frac{Area\ of\ failure\ (cm^2)}{Total\ area\ (cm^2)} \times 100\% \quad (12)$$

where *Pmax* is the load when the sample breaks (N) and *A* is the strain area (mm^2).

2.5 Data Analysis

Data analysis was analyzed using IBM Statistics 26 Software with a completely randomized design on two test phases. There is an influence of wood species (puspa wood and coconut trunk) on wettability adhesive and layer combination (PPP, CCC, PCP, and CPC) on the characteristics of CLT. The influence of factors on observation was tested at 95% confidence, and Duncan's Multiple Range Test (DMRT) was carried out to determine the difference between the levels of the factor that affected the response.

3. Results and Discussion

3.1. Characteristics of Polyurethane Adhesive

3.1.1. Solid content and gelation time

The solids content is the solid resin content that does not evaporate during the heating process. The solids content obtained in this study is shown in **Table 1**. Isocyanate has the highest solids content of 99.47%, while polyols have the lowest solids content of 86.73%. The solid content of PU adhesive was 96.95%. The PU adhesive in this study had different solids content from its constituent materials. The research of García-Pacios et al. (2011) and Liu et al. (2019) also showed that the solids content of PU adhesives varies depending on the constituent materials. Hass et al. (2012) reported that the solids content of PU adhesive could reach 100%. Adhesives with the highest solids content show high resin content directly proportional to the molecular weight, viscosity, and specific gravity. High solids content can increase the adhesive's entrance into the wood to form an optimal bond (Yuniarti et al. 2020).

Table 1. The solids content of isocyanate, polyol, and PU adhesive and the gelation time of the PU adhesive

Parameter	Value
Solids content (%)	
Isocyanate	99.47
Polyol	86.73
PU Adhesive	96.95
Gelation Time (minute: 25 °C)	161.8

Gelation time indicates the time required for the adhesive to thicken or become a gel at a specific temperature. Gelation time is the maximum period the adhesive is in an adequate fluid state to be applied to the substrate (Kong et al. 2011). The result of testing the gelation time on PU adhesive is 116.8 minutes. This time is still within the pressing time of the CLT manufacturing process in this study, which is 200 minutes. Therefore, PU adhesive can be used to manufacture CLT in this study.

3.1.2. Viscosity

Viscosity is the ability of the adhesive to flow from one surface to another on the glued wood to form a continuous and evenly spreadable layer. Viscosity will affect the adhesive penetration process on wood (Eskani et al. 2017). The viscosity results in this study are shown in **Fig. 2.** The mean viscosity of isocyanates ranged from 200.29-212.38 mPa.s, polyols ranged from 122.95-127.22 mPa.s and PU adhesives ranged from 712.01-1524.45 mPa.s (**Fig. 2**). The viscosity of PU is higher than its constituent materials. The PU adhesive bonds between isocyanates and polyols could cause it. The viscosity of the PU adhesive in this study was higher than that of the commercial PU adhesive, which was 150-250 mPa.s. It might be because this study's PU adhesive has a higher molecular weight (NCO/OH ratio is 1.5/1) than commercial PU adhesives (NCO/OH ratio is 1/1). Increasing the molecular weight of the PU adhesive will increase its viscosity (Szycher 2013).

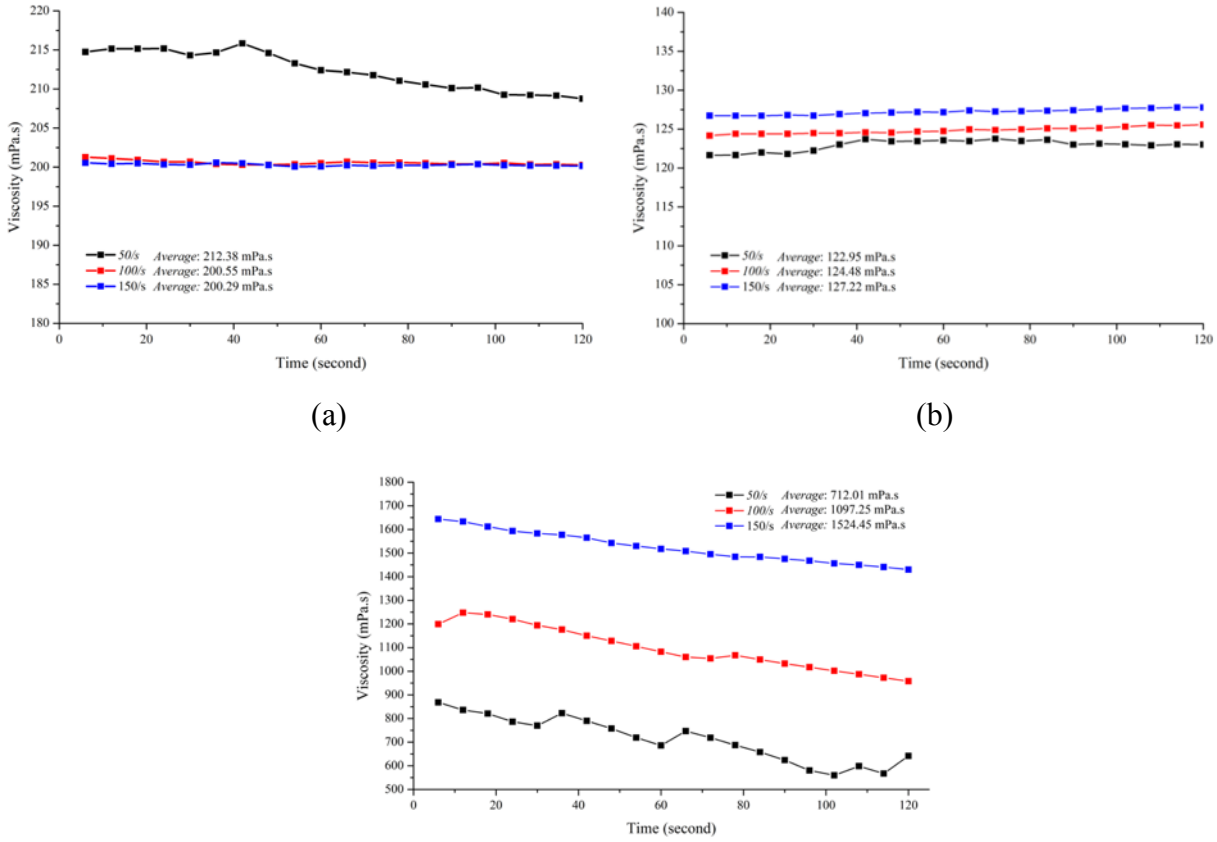

Fig. 2. Viscosity of isocyanates (a), polyols (b), and PU adhesive (c) on various speed rotations.

3.1.3. Analysis of functional group-FTIR

FTIR analysis can identify the functional groups in the adhesive. Functional group analysis was carried out under liquid and hardened adhesive conditions. **Fig. 3** shows the characteristics of the FTIR spectra of MDI, polyol, liquid PU, and solid PU, while the details of functional groups are shown in **Table 2.**

The wavenumber of 2869 cm^{-1} wave shows the C-H strain; at that wavenumber, the polyol intensity is higher than the others. The wavenumber of 2248 cm^{-1} indicates the NCO group that does not react to the PU adhesive in either the liquid or solid state. The PU solid has a lower

intensity than the PU liquid. It might be due to the reduced content of NCO groups in the solid condition of the adhesive. The peak at the wavenumber 1727 cm^{-1} is the strain of the urethane carbonyl group (C=O), which showed the presence of a urethane structure in the PU adhesive (Cui et al. 2017). The wavenumber of 1507 cm^{-1} shows strong urethane bonding in MDI, liquid PU, and solid PU samples. The wavenumber of 1272 cm^{-1} indicates the C-N functional group (Amide II band). The absorption peak at wavenumber 1103 shows the representation of secondary O-H groups (Kong et al. 2011), and the polyol has the highest intensity at that wavenumber.

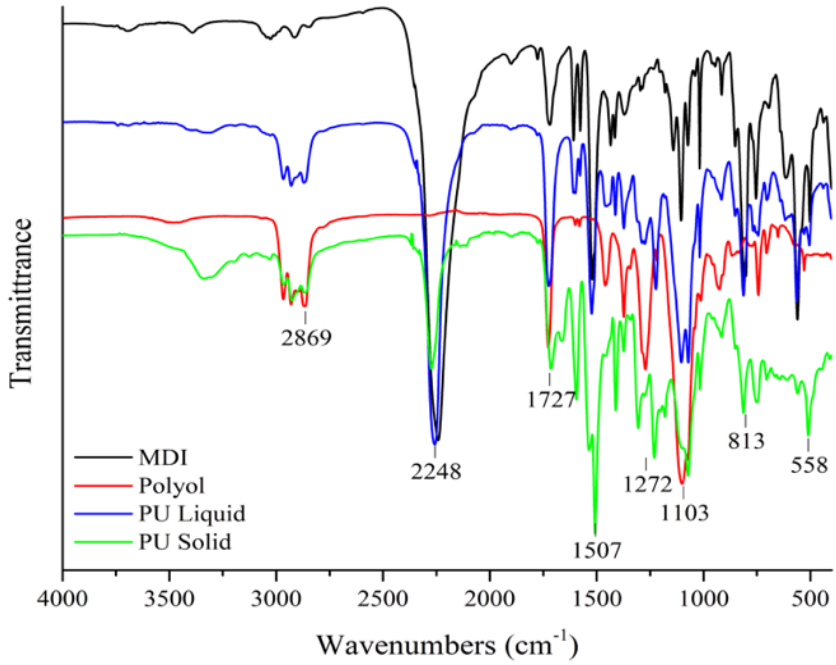

Fig. 3. Analysis of functional group-FTIR.

Table 2. The result of FTIR analysis in isocyanates, polyols, liquid PU, and solid PU

Wavenumber (cm^{-1})				Functional Group	References
Isocyanates	Polyols	PU Liquid	PU Solid		
2869	2869	2869	2869	C-H	2800-3000 cm^{-1} (Gurunathan et al. 2015)
2248	-	2248	2248	N=C=O	2230-2276 cm^{-1} (Poh et al. 2014; Oliviero et al. 2019)
1727	1727	1727	1727	C=O	1664-1780 cm^{-1} (Gurunathan et al. 2015)
1507	1507	1507	1507	Urethane bond	1460-1600 cm^{-1} (Thébault et al. 2015)
1272	1272	1272	1272	C-N (Amide II band)	1200-1500 cm^{-1} (Sunija et al. 2014)
1103	1103	1103	1103	Secondary O-H	1100-1200 cm^{-1} (Hazmi et al. 2013; Kong et al. 2011)

3.1.4. Analysis of GCMS

The results of the GCMS analysis on PU adhesive are presented in **Fig. 4** and **Table 3**. The highest peak was found at 27.8 minutes, indicating benzeneethanamine, N,α-dimethyl- and 3-furaldehyde compounds. At 24.80 minutes, propylamine compounds were shown, and at 2.60 minutes, acetonitrile compounds were shown.

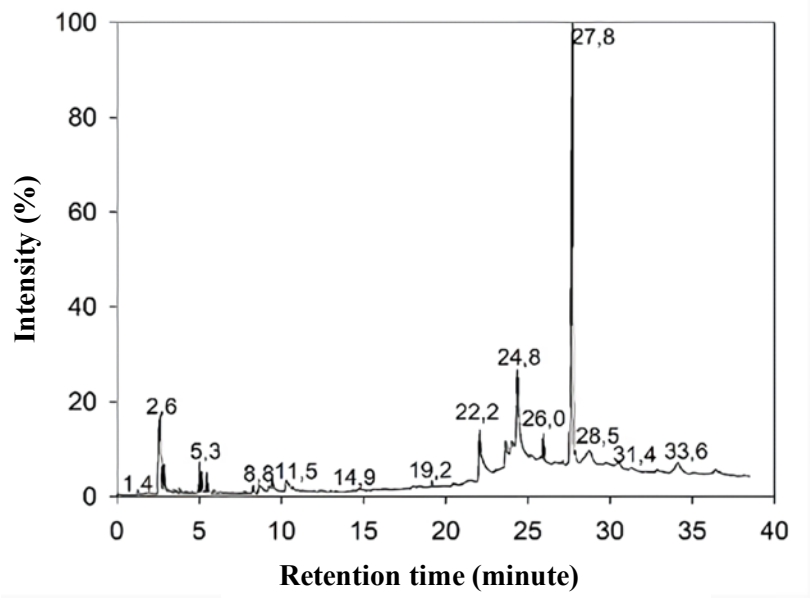

Fig. 4. Analysis of Py-GCMS.

Table 3. Result of analysis Py-GCMS

Peak Number	Retention (minute)	Molecular Weight (m/z)	Compound
1	2.54	44	Carbon dioxide
2	2.62	41	Acetonitrile
3	2.88	43	Ethylenimine
4	3.52	43	Ethylenimine
5	3.80	43	Ethylenimine
6	5.01	70	1-Pentene
7	5.16	45	Ethylamine
8	5.48	43	Ethylenimine
9	5.91	59	Propylamine and Methylamina, N,N-dimethyl-
10	8.28	59	Propylamine and Methylamina, N,N-dimethyl-
11	9.44	58	2-Propen-1-ol
12	10.28	106	Karbonothioik dihydrasida
13	10.38	59	Methylamina, N,N-dimethyl-
14	10.49	59	Methylamina, N,N-dimethyl-
15	19.18	105	2-Amino-2-methyl-1,3-propanediol and Diethanolamine
16	22.08	43	Ethylenimine
17	22.35	73	1-Butanamine, Isobutilamine, and 2-Propanamina, N-methyl-
18	23.65	198	N-Nitrosodiphenylamine
19	24.02	55	Propanenitrile
20	24.36	198	N-Nitrosodiphenylamine
21	25.16	212	Benzoic acid, 2-phenylhydrazide
22	25.94	57	Methane, isocyanato-
23	27.10	149	Benzeneethanamine, N,α-dimethyl-
24	27.72	149	Benzeneethanamine, N,α-dimethyl-
25	28.72	239	Benzenamine, N,N-dimethyl-4-[(3-methylphenyl)azo]-
26	30.50	43	Ethylenimine
27	32.83	57	Methane, isocyanato-
28	34.12	239	Acetamide, N-9H-fluoren-2-yl-N-hydroxy-
29	36.41	96	3-Fureldehyde
30	36.66	95	2(1H)-Pyridinone

Notes: identification of the compound based on previous studies (Dyer and Junior 1958; Dyer and Read 1961; Dyer and Wright 1959; Zhang et al. 2009).

The results of Py-GCMS were a form of polyurethane formation and degradation. The reaction for the formation of polyurethane is as follows:

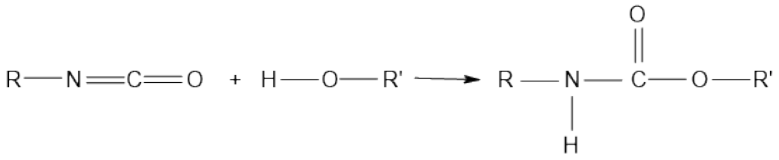

(1)

According to Scheme 1, the formation reaction is characterized by peaks number 22 and 27 (—N=C=O) and peak number 28 (—OH), which form polyurethane with urethane and several forms of degradation, including Schemes 2-4.

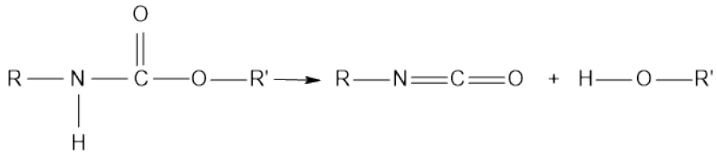

(2)

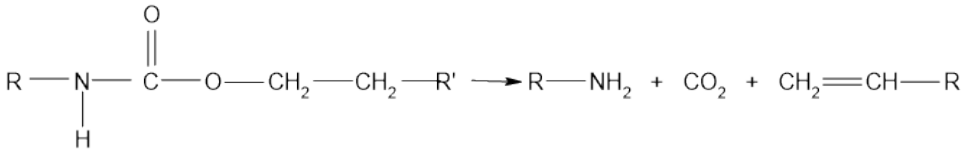

(3)

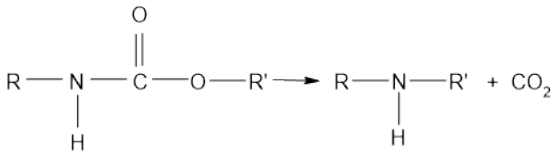

(4)

Peak numbers 22 and 27 (—N=C=O), peaks number 6 and 29 (chain O), and peak number 28 (—OH) indicate the degradation product of polyurethane (Scheme 2). In addition, peak numbers 3, 4, 5, 7, 8, 9, 10, 13, 14, 15, 17, and 26 (—NH2); peak numbers 2, 18, 20, 21, and 25 (N chain); peak numbers 21, 16, 23, and 24 (—NH—); and peak number 1 (O=C=O) indicates the degradation product of polyurethane (Scheme 3 and Scheme 4). However, the CH2=CH bond was not indicated in the Py-GCMS results in this study.

3.1.5. Dynamic Mechanical Analysis (DMA)

Dynamic Mechanical Analysis (DMA) analyzes mechanical and viscoelastic behavior under thermodynamic changes. DMA provides information on adhesive hardening, vitrification, and gelatinization, which is essential for the preparation, modification, and use of adhesives (Lei and Frazier 2015). **Fig. 5** and **Fig. 6** show the results of DMA testing on PU adhesives.

DMA test results provide information related to storage modulus (E'), loss modulus (E"), and tan delta data correlated to the thermo-mechanical and viscoelastic properties of adhesives. The highest value of E' is at a temperature of 28.75°C, 111.69 GPa (**Fig. 5**). The value of E' decreased during heating starting from 30–60°C. However, the value of E" and tan delta increased at that temperature. The same phenomenon occurs in other synthetic adhesives. The value of E' in PF adhesive decreased starting from 125°C because the adhesive softened (Hong et al. 2018). The PU adhesive decreased the value of E' at a lower temperature than the PF adhesive. This tendency indicates that the PU adhesive has high reactivity at lower temperatures.

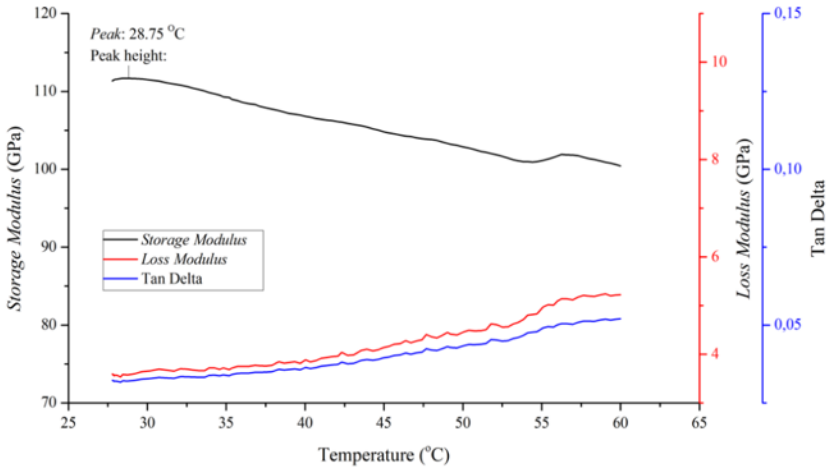

Fig. 5. Termo-mechanical analysis of PU adhesive.

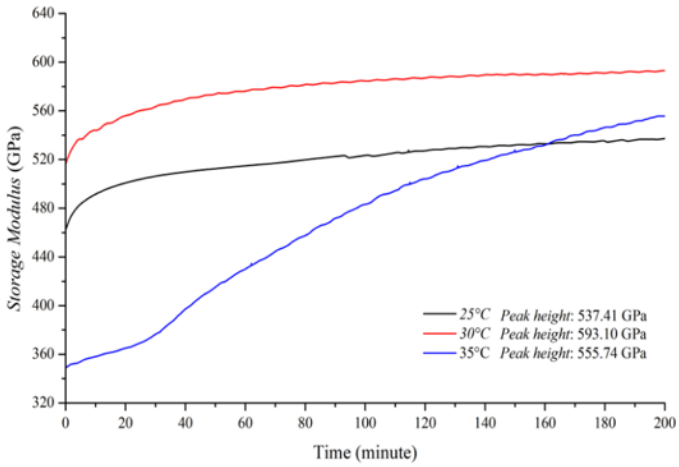

Fig. 6. Thermo-mechanical analysis of PU adhesive at various temperatures.

Thermo-mechanical analysis of PU adhesive at different temperatures for 200 minutes aims to determine the optimum temperature used in the CLT manufacturing process. The value of E' at each temperature is 537.41 GPa, 593.1 GPa, and 555.74 GPa (**Fig. 6**). The highest value of E' is found at 30°C. This result shows that the optimum temperature in the CLT manufacturing process is 30°C. Luedtke et al. (2015) also reported that PU adhesive is an adhesive that hardens quickly at room temperature.

3.2. Characteristics of Material for CLT

The wood characteristics of CLT material will affect the bond quality of the resulting CLT. Various raw materials have different wood characteristics, affecting the CLT's characteristics (Hovanec 2015; Yusoh et al. 2021). **Table 4** shows the physical characteristics of the puspa wood and coconut trunk used in this study. The specific gravity of puspa wood is 0.57 (heartwood) and 0.53 (sapwood), and the coconut trunk is 0.63. The specific gravity of puspa wood and coconut has met the raw material requirements for CLT, which is 0.35 (ANSI 2018). The dry density of puspa wood is 0.71 g.cm^{-3} (heartwood), 0.70 g.cm^{-3} (sapwood), and the coconut trunk is 0.78 g.cm^{-3}. The specific gravity and density of the coconut trunk are higher than that of puspa wood.

The ANOVA result showed that the wood species significantly affected the specific gravity and density. Differences can influence the anatomical structure of the two types of wood. Puspa wood has an anatomical structure of solitary and diffuse pore type (Martawijaya et al. 1989), while coconut has an anatomical structure of vascular bundles type (Fathi and Frühwald 2014). The density of the wood from different species will affect the character of the resulting product (Machado et al. 2014). Wood has a high density has high mechanical properties.

Table 4. Physical properties of the raw material for CLT

Characteristics	Puspa (Heartwood)	Puspa (Sapwood)	Coconut
Specific gravity	0.57 ± 0.02^{a}	0.53 ± 0.01^{b}	0.63 ± 0.003^{c}
Density ($g.cm^{-3}$)			
Air dried	0.71 ± 0.01^{a}	0.70 ± 0.03^{b}	0.78 ± 0.08^{c}
Oven-dried	0.72 ± 0.02^{a}	0.69 ± 0.03^{b}	0.77 ± 0.07^{c}
Moisture content (%)	15.82 ± 0.31^{a}	15.63 ± 0.47^{b}	12.65 ± 0.61^{c}
Shrinkage (%)	18.02 ± 3.58^{a}	14.11 ± 2.17^{b}	11.72 ± 1.98^{c}

Notes: Numbers in the same column followed by different letters mean significantly different values from the ANOVA results ($\alpha = 0.05$). Data is the average value of n = 5.

The moisture content of the CLT wood material in this study was 15.49% (heartwood of puspa), 15.63% (sapwood of puspa), and 12.65% (coconut trunk). Based on these data, puspa wood and coconut trunk have met the raw material requirements for CLT, which is ±15% (ANSI 2018). The ANOVA result showed that the wood species significantly affected the moisture content of material CLT. The shrinkage of puspa heartwood was 18.02%, puspa sapwood was 14.11%, and coconut was 11.72% (**Table 4**). The shrinkage value of CLT wood material can affect the resulting CLT dimension panels. The ANOVA result showed that the wood species significantly affected the shrinkage of material CLT. Coconut has a lower shrinkage than puspa. It might be due to coconut's lower water content than puspa. The value of shrinkage is also influenced by the extractive content contained in the wood. The extractive content in puspa wood and coconut is shown in **Table 5.**

The extractives content dissolved in cold water, hot water, and 1% NaOH in puspa wood were 6.06%, 7.24%, and 14.68%. The extractives content dissolved in cold water, hot water, and 1% NaOH in coconut trunk were 14.18%, 11.19%, and 22.72%. The pH value of puspa wood is 6.11 and the coconut trunk is 7.36 (**Table 5**).

Table 5. Extractive content and pH material for CLT

Characteristics	Puspa	Coconut
Extractive content (%)		
Dissolved in cold water	6.06 ± 0.43^{a}	14.18 ± 1.47^{b}
Dissolved in hot water	7.24 ± 0.51^{a}	11.19 ± 0.22^{b}
Dissolved in NaOH 1%	14.68 ± 0.78^{a}	22.72 ± 1.15^{b}
pH	6.11 ± 0.05^{a}	7.36 ± 0.22^{b}

Notes: Numbers in the same column followed by different letters mean significantly different values from the ANOVA results ($\alpha = 0.05$). Data is the average value of n = 5.

The ANOVA result showed that the wood species significantly affected the extractive content and pH value. The pH value and the presence of extractives in wood will affect wood's wettability, swelling, and shrinkage (Jankowska et al. 2018; Knorz et al. 2014; Pooryousefy et al. 2021; Roffael 2016). However, this study was inversely proportional between the effect of

extractives and pH on the rate of wettability. Lai et al. (2021) reported that the particle size of PU adhesive tends to be stable at pH 5-12. Therefore, the pH of Puspa and Coconut wood did not affect the wettability rate of the PU adhesive in this study. The wettability and surface roughness of puspa wood and coconut are shown in **Table 6**.

Table 6. Surface characteristics material for CLT

Characteristics	Puspa	Coconut
Surface roughness (μm)	8.76 ± 1.63[a]	11.38 ± 1.57[a]
Wettability value	0.14 ± 0.09[a]	0.23 ± 0.03[a]

The surface roughness of puspa wood is 8.76 m and coconut is 11.38 m (**Table 6**). The roughness of the coconut trunk is higher than that of puspa wood. Surface roughness will affect adhesive penetration. Kim et al. (2016) reported that surface roughness is correlated with wettability value. As shown in **Table 6**, the wettability value of coconut wood is higher than that of puspa wood. This result shows that the adhesion is better on coconut trunks compared to puspa wood. The adhesive will flow, fill the wood pores, and form a bond with the wood surface (Darmawan et al. 2018, 2020). Changes in the contact angle of PU adhesive on the surface of puspa wood and coconut trunk are shown in **Fig. 7**. In the initial drop, the contact angle diminishes quickly, followed by a continuous decline until consistent at a specific time. The decrease in contact angle on the coconut trunk is sharper than that of puspa wood. This tendency shows that PU adhesive can penetrate well on coconut trunks.

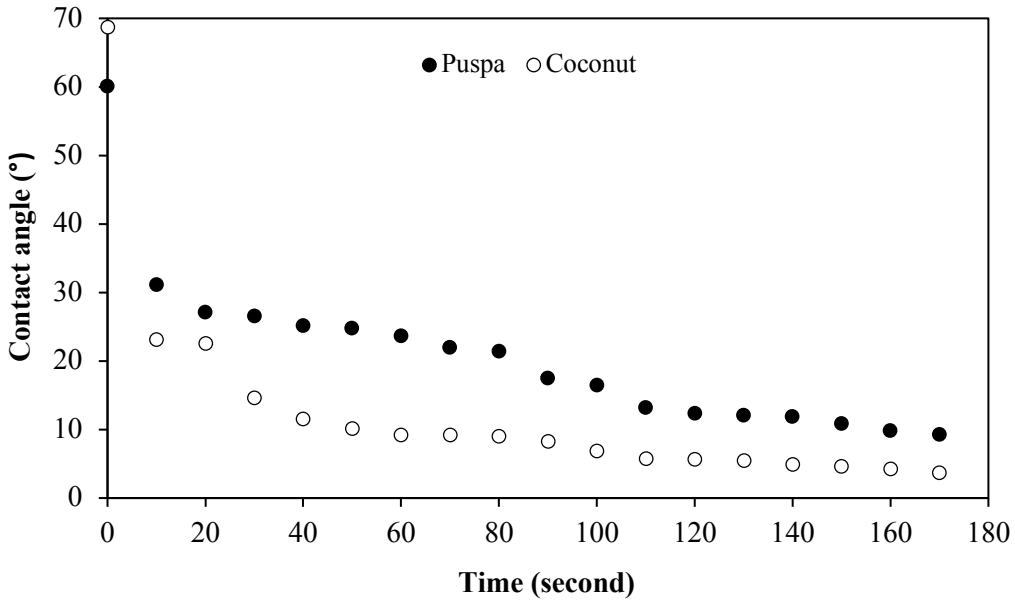

Fig. 7. Changes in contact angle of PU adhesive on time changes in puspa and coconut wood.

3.3. Characteristics of CLT

3.3.1. Density

The CLT density values ranged from 0.60-0.73 g.m^{-3} (**Fig. 8**). The lowest density value was found in the PPP CLT and the highest in the CCC CLT. The ANOVA result showed that the layer combination did not significantly affect the density values of CLT. This result shows that the CLT density in this study is relatively homogeneous. The density of the raw material determines the

density of CLT. The higher density of wood making up CLT, the higher the density of CLT panels produced (Lepage 2012; Srivaro et al. 2021). **Table 4** shows that coconut has a higher density and density than puspa wood. Therefore, CCC CLT has the highest density, followed by CPC, PCP, and PPP.

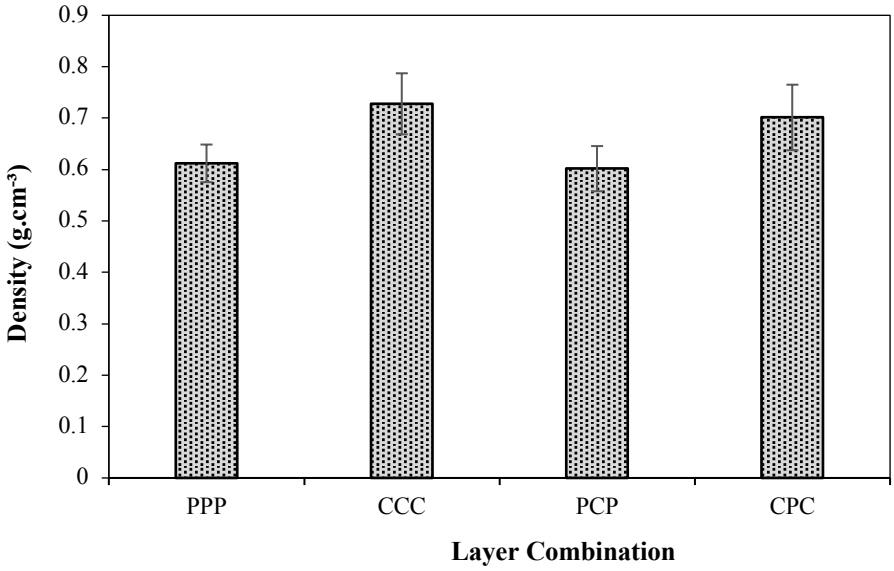

Fig. 8. Density value of CLT on various layer combinations.

3.3.2. Moisture content (MC)

The MC values of CLT ranged from 13.90 to 14.51% (**Fig. 9**). The lowest MC values were found in the CLT CPC and the highest in the CLT PPP. The MC CLT in this study has met the JAS 3079:2019 standard, which requires that the MC CLT panel is < 15%. The ANOVA result showed that the layer combination did not significantly affect the value of MC CLT. The MC of CLT will affect the modulus of elasticity and shear strength of the resulting CLT (Gülzow et al. 2011).

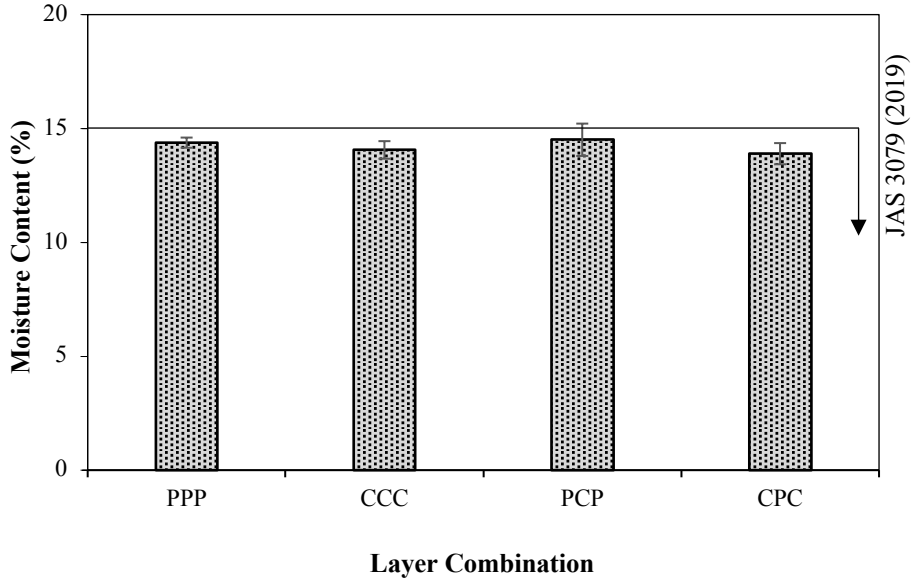

Fig. 9. Moisture content value of CLT on various layer combinations.

3.3.3. *Volume shrinkage*

The volume shrinkage values of CLT ranged from 5.51–6.45% (**Fig. 10**). The lowest volume shrinkage value is found in the CCC CLT and the highest in the PPP CLT. The ANOVA result showed that the layer combination did not significantly affect the value of volume shrinkage CLT. The physical characteristics of the constituent materials influence the volume shrinkage values. **Table 4** shows that puspa has higher moisture content and shrinkage than coconut. In addition, the extractive content of puspa is higher than coconut (**Table 5**). Therefore, the highest shrinkage value was found in the PPP CLT, followed by the PCP, CPC, and CCC. However, the value was not significantly different from each other. This result shows that the puspa hybrid CLT is better than the PPP CLT, while the coconut single CLT has better quality than the hybrid CLT.

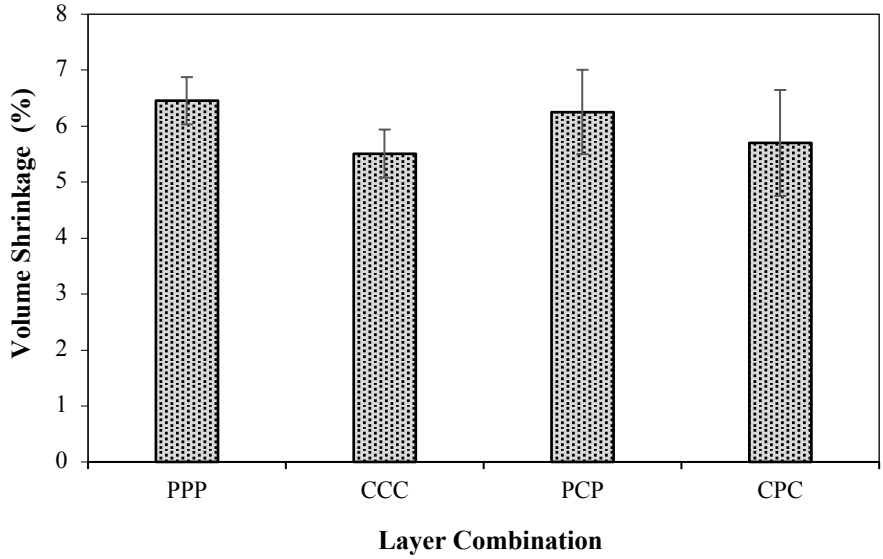

Fig. 10. Volume shrinkage value of CLT on various layer combinations.

3.3.4. *Water absorption (WA) and thickness swelling (TS)*

The WA values of CLT ranged from 16.50–19.83% (**Fig. 11**). The TS value of CLT obtained ranged from 0.68–3.43% (**Fig. 12**). The lowest WA and TS values were found in the CCC CLT and the highest in the PPP CLT. The ANOVA result showed that the layer combination significantly affected the value of TS CLT. DMRT results showed that the TS CLT values were significantly different at each level.

The dimensional stability of coconut is better than that of puspa wood. Research by Glass and Zelinka (2010) and Srivaro et al. (2021) reported that density significantly affects WA and TS. Low extractives can reduce the ability of composite products to absorb water (Sheshmani 2013; Sheshmani et al. 2012; Wang et al. 2018). Coconuts' surface roughness and wettability were higher than puspa wood (**Table 6**). This tendency shows that the adhesive quickly penetrates and forms bonds with wood (Darmawan et al. 2018, 2020). Therefore, the value of WA and TS CCC CLT is lower than CLT CPC, the value of WA and TS CPC CLT is lower than PCP CLT, and the value of WA and TS PCP CLT is lower than PPP CLT. Based on this, CLT from puspa wood will be of good quality when combined (hybrid CLT). However, single CLT of coconut is better than hybrid CLT, showing that the CLT CCC is significantly different from other CLT.

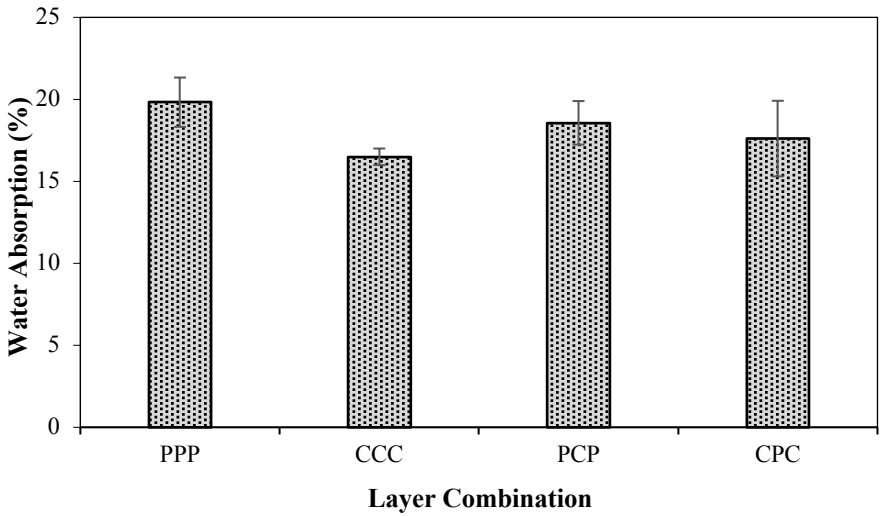

Fig. 11. WA value of CLT on various layer combinations.

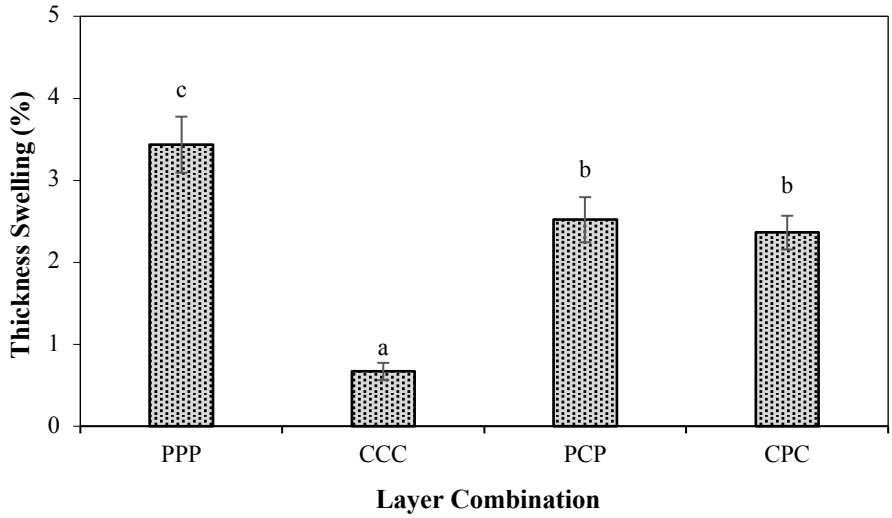

Fig. 12. TS value of CLT on various layer combinations (The different letters showed a significant difference).

3.3.5. Delamination

The value of water delamination ranged from 22.46-56.41% and boiling delamination ranged from 26.54–67.84% (**Fig. 13**). The lowest value of water and boiling delamination was found in CLT CCC, and the highest was found in CLT PPP. The ANOVA result showed that the layer combination significantly affected the water and boiling delamination values. The water and boiling delamination value of CLT PCP and CPC is lower than CLT PPP. However, in contrast to coconut, the CLT CCC is lower than its hybrid CLT. It could be caused by the different characteristics of the two types of wood (**Table 4-6**). Differences in wood characteristics can affect the characteristics of the resulting CLT (Hovanec 2015; Srivaro et al. 2021; Yusoh et al. 2021).

The overall delamination value in this study did not meet the JAS 3079:2019 standard, which requires that the maximum of CLT delamination is 10% (**Fig. 13**). Previous studies have also reported that CLT using PU adhesive with other wood types has a high delamination value. During the curing process, PU adhesive tends to foam due to the reaction between the polyether and the active isocyanate group (Na et al. 2005). The foam can form a void in the bond line, causing the

bonding to weaken (Thomson 2004). Delamination of CLT made from acacia wood was 36.29% and 70.80% (Yusof et al. 2019b; a). Brunetti et al. (2020) reported that the delamination of CLT made of beech wood could reach 98.50%.

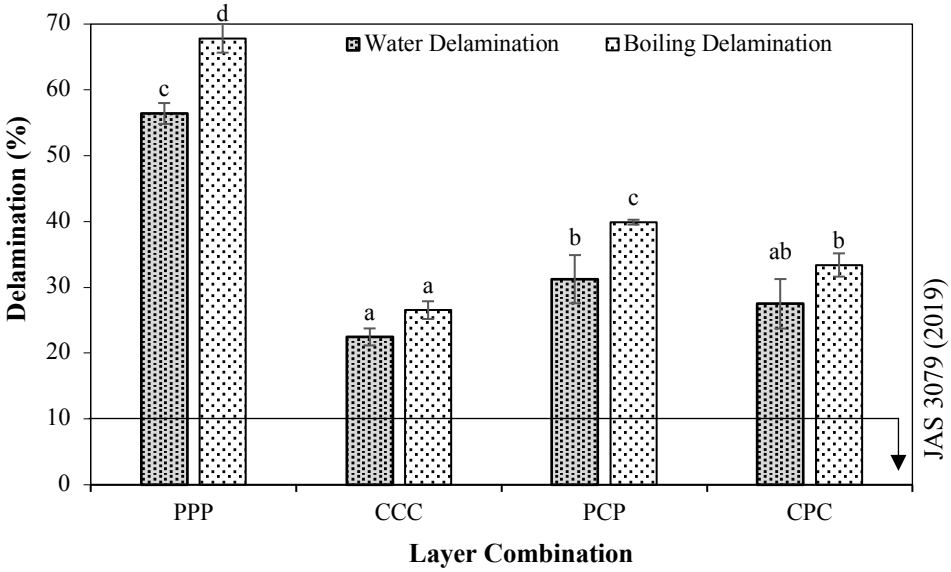

Fig. 13. Delamination value of CLT on various layer combinations (The different letters showed a significant difference).

3.3.6. Modulus of Elasticity (MOE) and Modulus of Rupture (MOR)

The value of MOE CLTs ranged from 26159–36838 MPa (**Fig. 14**). The lowest was found in PPP CLT and the highest in CPC CLT. The ANOVA result showed that the layer combination significantly affected the value of MOE CLT. The value of MOR CLTs ranged from 40–44 MPa (**Fig. 15**). The lowest was found in PPP CLT and the highest in CPC CLT. The ANOVA result showed that the layer combination did not significantly affect the value of MOR CLT.

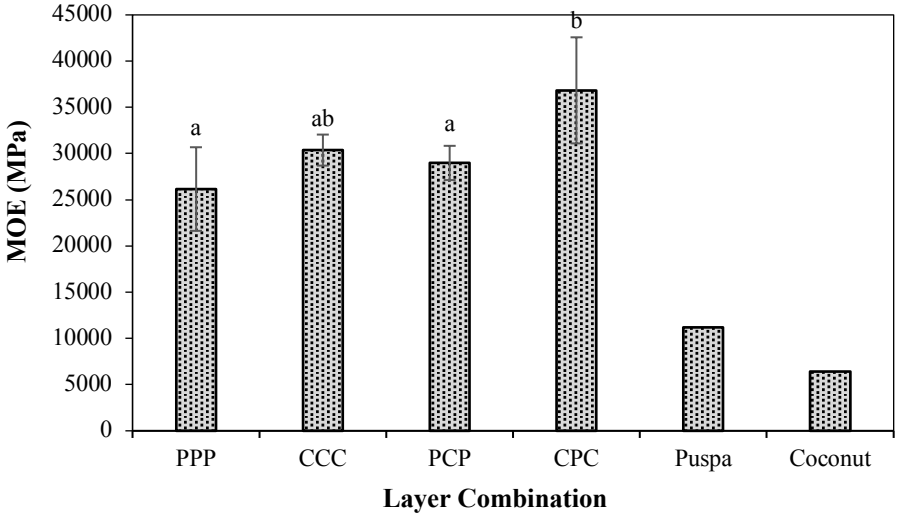

Fig. 14. MOE value of CLT on various layer combinations (The different letters showed a significant difference).

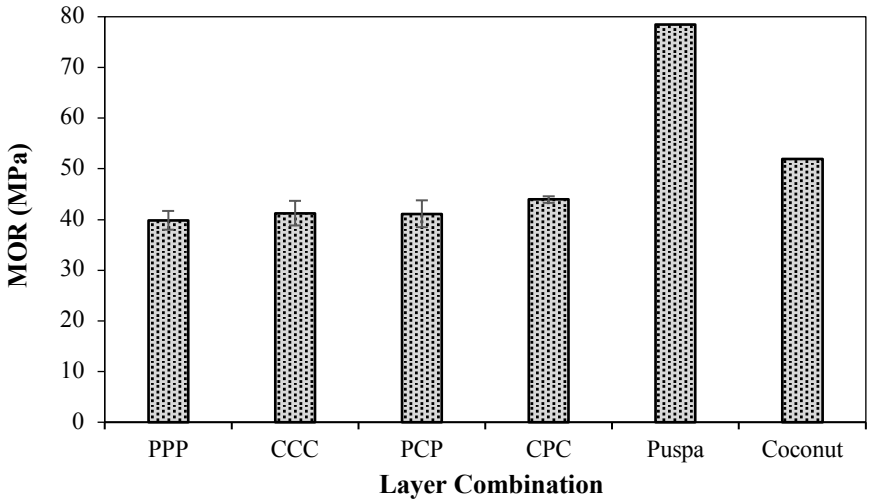

Fig. 15. MOR value of CLT on various layer combinations.

The hybrid CLT had higher MOE and MOR values than single CLT in puspa wood and coconut trunk. This result is in line with previous studies which reported that hybrid CLTs had better mechanical properties than single CLTs (Aicher et al. 2016; Corpataux et al. 2020; Hematabadi et al. 2021). The characteristics of two types of wood affect the quality of the CLT. As shown in **Table 6**, the surface roughness of the coconut trunk was higher than puspa. Surface roughness will affect adhesive penetration (Kim et al. 2016). Therefore, the MOE and MOR values of CLT composed from coconut trunk were higher than CLT composed from puspa wood. The MOE value of puspa wood was 11179 MPa; for coconut, the trunk was 6381 MPa, while the MOR for puspa wood was 78 MPa and for coconut was 52 MPa (Mardikanto et al. 2017; Srivaro et al. 2020). Overall the MOE value of CLT is higher than that of solid wood (**Fig. 14**). However, the MOR value of CLT is lower than that of solid wood (**Fig. 15**). This is because the CLT has an adhesive connection (Mardikanto et al. 2017). The failure of PPP CLT is more severe than the others (**Fig. 16**). Some failures that occurred are in the form of damage to the bond line.

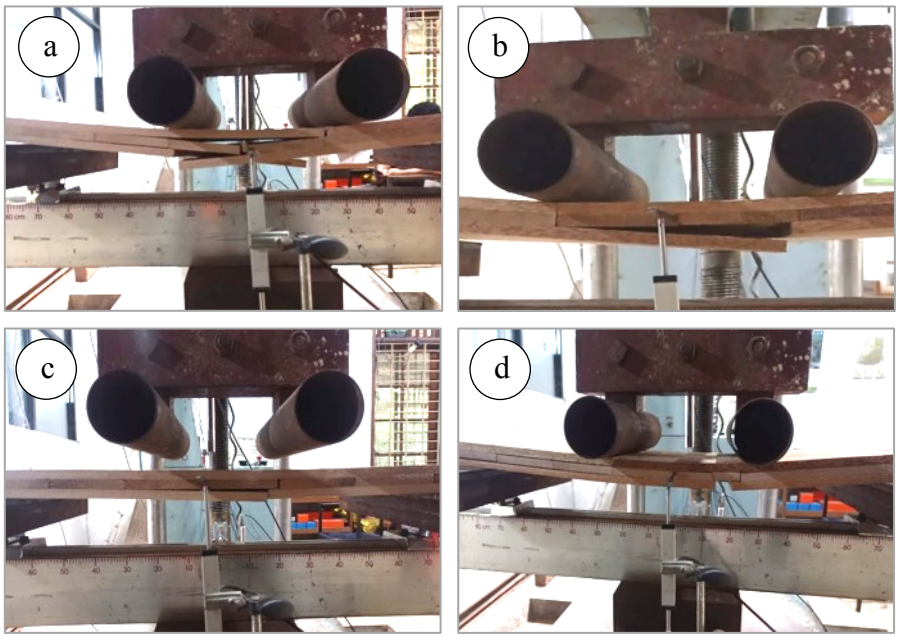

Fig. 16. Failure at the samples due to MOE and MOR testing: (a) PPP CLT, (b) CCC CLT, (c) PCP CLT, and (d) CPC CLT.

3.3.7. *Shear strength*

Fig. 17 and **Fig. 18** show the stress-strain graph due to the shear load for each CLT sample. There was a tremendous distinction in the stress-strain graph between the repeats. It might be due to the difference in the shear strength value and the type of failure in each sample.

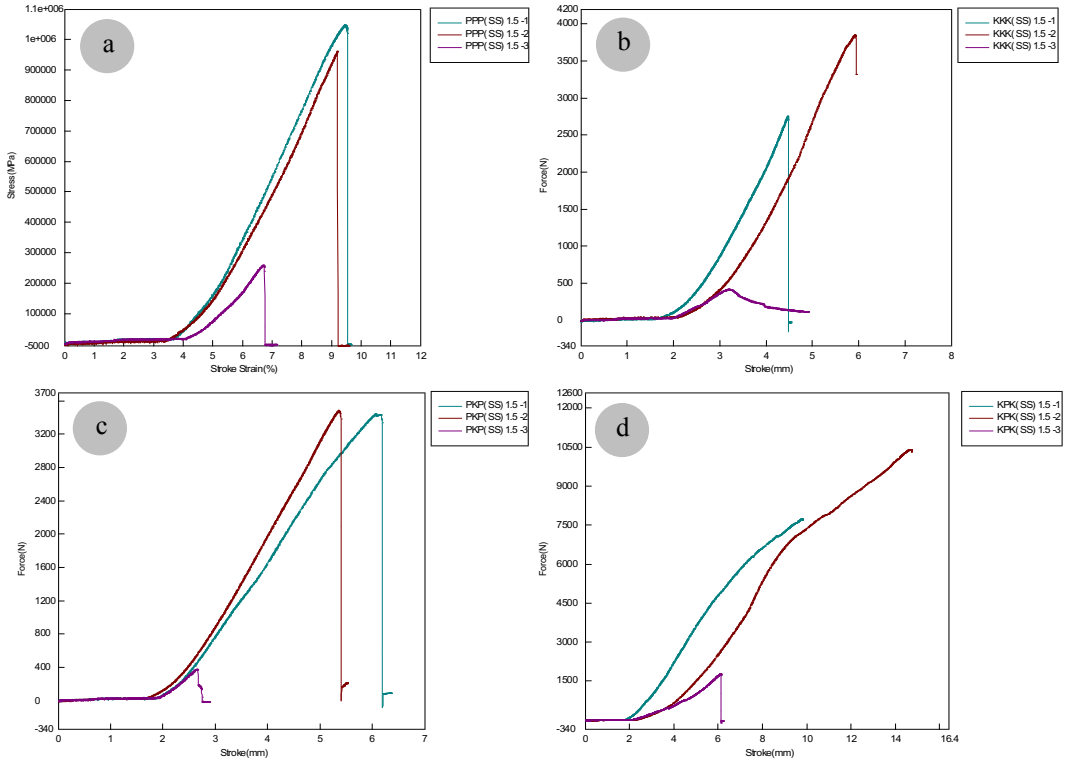

Fig. 17. Shear stress-strain graph parallel to the grain direction of (a) PPP CLT, (b) CCC CLT, (c) PCP CLT, and (d) CPC CLT.

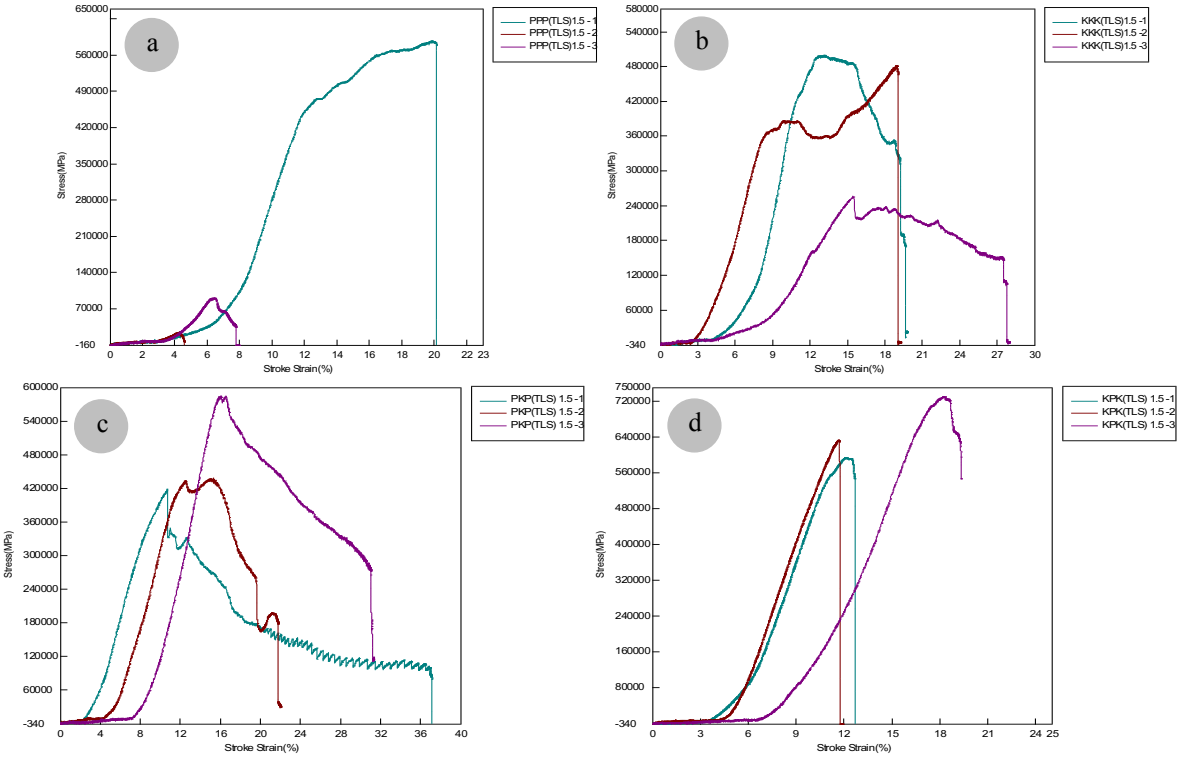

Fig. 18. Shear stress-strain graph perpendicular to the grain direction of (a) PPP CLT, (b) CCC CLT, (c) PCP CLT, and (d) CPC CLT.

The shear strength parallel to the grain direction values for PPP CLT was 1.49 MPa, CCC CLT was 1.82 MPa, PCP CLT was 1.93 MPa, and CPC CLT was 5.23 MPa. The shear strength perpendicular to the grain direction values for PPP CLT was 0.59 MPa, CCC CLT was 1.01 MPa, PCP CLT was 1.17 MPa, and CPC CLT was 1.64 MPa (**Fig. 19**). The ANOVA results showed that the layer combination did not have a significant effect on the shear strength parallel and perpendicular to the grain direction.

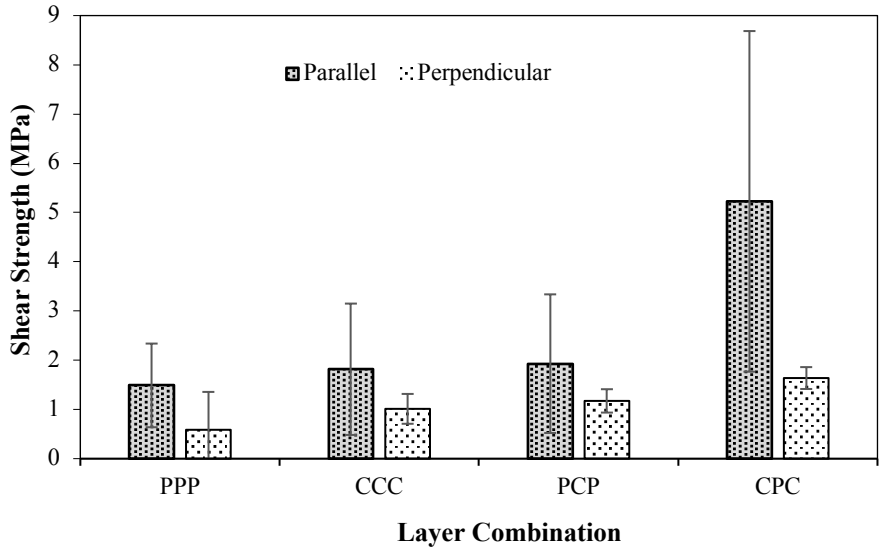

Fig. 19. Shear strength parallel and perpendicular to the grain direction value of CLT on various layer combinations.

Hybrid CLT had higher shear strength values than single CLT in puspa wood and coconut trunk. This result shows that hybrid CLT is better than single CLT. Previous studies reported that hybrid CLTs had better mechanical properties than single CLTs (Aicher et al. 2016; Corpataux et al. 2020; Hematabadi et al. 2021). The value of shear strength parallel and perpendicular to the grain direction of CLT made from coconut trunk was higher than that of CLT made from puspa wood. It could be caused that CLT quality depends on the constituent materials' characteristics (Srivaro et al. 2021; Yusoh et al. 2021). **Table 4-6** shows that the characteristics of the coconut trunk are better than puspa, so CLT made from coconut trunk is better than CLT made from puspa wood.

Fig. 20 and **Fig. 21** show the failure of the shear test results. PPP CLT failed on the bond line in the shear parallel and perpendicular to the grain direction tested. The panel of CCC CLT, PCP, and CPC CLT suffered a wood failure in both the shear parallel and perpendicular to the grain direction tested. This result shows that puspa wood has poor adhesive penetration.

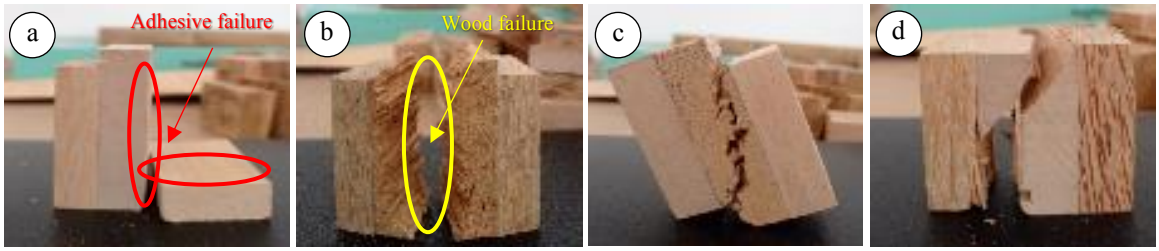

Fig. 20. Failure at the samples due to block shear parallel to the grain direction testing: (a) PPP CLT, (b) CCC CLT, (c) PCP CLT, and (d) CPC CLT.

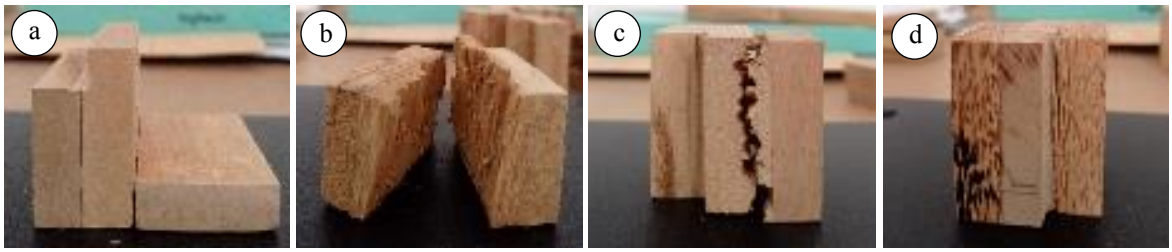

Fig. 21. Failure at the samples due to block shear perpendicular to the grain direction testing: (a) PPP CLT, (b) CCC CLT, (c) PCP CLT, and (d) CPC CLT.

The success of shear strength in CLT is explained by the percentage of wood failure of at least 90% (JAS 2019). **Table 7** shows the evaluation of failure from the shear strength test results. On average, the entire sample did not meet the JAS 3079 (2019) standard. However, the individual samples contained CLT that met the standard. A total of two samples of CCC CLT and two of CPC CLT in the shear strength test perpendicular to the grain had a percentage of wood failure of 100%. The results of the shear strength test parallel to the grain with 100% wood damage percentage are CCC CLT with one sample, PCP and CPC CLT with two samples. This result shows that hybrid CLT can improve the quality of single CLT in terms of its mechanical strength.

Table 7. Failure evaluation of shear strength test results

Layer Combination of CLT	Percentage of Wood Failure (JAS 3079:2019 (≥ 90%))	
	Shear Strength (//)	Shear Strength (⊥)
PPP	33.33	0
CCC	60.67	66.67
PCP	66.67	66.67
CPC	66.67	33.33

Notes: // = parallel to the grain direction, ⊥ = perpendicular to the grain direction.

4. Conclusions

The PU adhesive used in this study had a solids content of 96.95%, gel time was 116.8 minutes, viscosity at each rotation speed was 712.01 mPa.s (50/s), 1097.25 mPa.s (100/s), and 1524.45 mPa.s (150/s). FTIR functional group analysis and analysis of Py-GCMS showed the spectra of the presence of NCO and OH bonds. The Dynamic Mechanical Analysis (DMA) test results show that the polyurethane adhesive could curr optimally at a temperature of 30°C for 200 minutes. The results of testing the characteristics of CLT wood material showed that the puspa wood and coconut trunk had different physical and chemical properties but had similar wettability to polyurethane adhesives. Coconut trunk CLT's physical and mechanical characteristics were better than puspa CLT. However, all CLT samples did not meet the JAS 3079 (2019) delamination standard. Based on the overall test results, the puspa hybrid CLT is better than the single CLT. In contrast to the coconut trunk in several parameters, the single CLT was better than the hybrid CLT.

Acknowledgments

This study was a part of RIIM-PRN project No. 65/II.7/HK/2022 titled "*Pengembangan Produk Oriented Strand Board Unggul dari Kayu Ringan dan Cepat Tumbuh dalam Rangka*

Pengembangan Produk Biokomposit Prospektif". The authors express their most profound appreciation to the late Prof. Dr. Fauzi Febrianto, without whom this project would never have been possible.

References

Aicher, S., Hirsch, M., and Christian, Z. 2016. Hybrid cross-laminated timber plates with beech wood cross-layers. *Construction and Building Materials* Elsevier Ltd 124: 1007–1018. DOI: 10.1016/j.conbuildmat.2016.08.051

American National Standards Institute (ANSI). 2018. ANSI/APA PRG 320-2018: *Standard for Performance-Rated Cross-Laminated Timber*. Tacoma (WA): APA - The Engineered Wood Association.

American Society for Testing Materials (ASTM). 2014. Standard Test Methods for Small Clear Specimens of Timber - D143. *ASTM International* 31. DOI: 10.1520/d0143-14.2

Aristri, M. A., Lubis, M. A. R., Laksana, R. P. B., Falah, F., Fatriasari, W., Ismayati, M., Wulandari, A. P., Nurindah, and Ridho, M. R. 2021. Bio-Polyurethane Resins Derived from Liquid Fractions of Lignin for the Modification of Ramie Fibers. *Jurnal Sylva Lestari* 9(2): 223-238. DOI: 10.23960/jsl29223-238

Brunetti, M., Nocetti, M., Pizzo, B., Negro, F., Aminti, G., Burato, P., Cremonini, C., and Zanuttini, R. 2020. Comparison of Different Bonding Parameters in the Production of Beech and Combined Beech-Spruce CLT by Standard and Optimized Tests Methods. *Construction and Building Materials* 265: 120168. DOI: 10.1016/j.conbuildmat.2020.120168

Corpataux, L., Okuda, S., and Kua, H. W. 2020. Panel and Plate Properties of Cross-Laminated Timber (CLT) with Tropical Fast-Growing Timber Species in Compliance with Eurocode 5. *Construction and Building Materials* 261: 119672. DOI: 10.1016/j.conbuildmat.2020.119672

Cui, S., Luo, X., and Li, Y. 2017. Synthesis and Properties of Polyurethane Wood Adhesives Derived from Crude Glycerol-Based Polyols. *International Journal of Adhesion and Adhesives* 79: 67–72. DOI: 10.1016/j.ijadhadh.2017.04.008

Darmawan, W., Ginting, M. B., Gayatri, A., Putri, R. L., Lumongga, D., and Hasanusi, A. 2020. Influence of Surface Roughness of Ten Tropical Woods Species on Their Surface Free Energy, Varnishes Wettability and Bonding Quality. *Pigment and Resin Technology* 49(6): 441–447. DOI: 10.1108/prt-01-2020-0005

Darmawan, W., Nandika, D., Noviyanti, E., Alipraja, I., Lumongga, D., Gardner, D., and Gérardin, P. 2018. Wettability and Bonding Quality of Exterior Coatings on Jabon and Sengon Wood Surfaces. *Journal of Coatings Technology and Research* 15(1): 95–104. DOI: 10.1007/s11998-017-9954-1

Dyer, E., and Junior, G. E. N. 1958. Thermal Degradation of Carbamates of Methylenebis-(4-phenyl Isocyanate). *Journal of the American Chemical Society* 888(4): 5495–5498. DOI: 10.1021/ja01553a045

Dyer, E., and Read, R. E. 1961. Thermal Degradation of O-1-Hexadecyl N-1-Naphthylcarbamates and Related Compounds. *Journal of Organic Chemistry* 26(11): 4388–4394. DOI: 10.1021/jo01069a050

Dyer, E., and Wright, G. C. 1959. Thermal Degradation of Alkyl N-Phenylcarbamates. *Journal of the American Chemical Society* 81(9): 2138–2143. DOI: 10.1021/ja01518a030

Eskani, I. N., Perdana, A., Eskak, E., and Sumarto, H. 2017. Getah Pohon Kudo (*Lannea coromandelica*) sebagai Alternatif Perekat untuk Produk Kerajinan. *Dinamika Kerajinan dan Batik: Majalah Ilmiah* 34(1): 19. DOI: 10.22322/dkb.v34i1.2265

Fathi, L., and Frühwald, A. 2014. The Role of Vascular Bundles on the Mechanical Properties of Coconut Palm Wood. *Wood Material Science and Engineering* 9(4): 214–223. DOI: 10.1080/17480272.2014.887774

García-Pacios, V., Iwata, Y., Colera, M., and Miguel Martín-Martínez, J. 2011. Influence of the Solids Content on the Properties of Waterborne Polyurethane Dispersions Obtained with Polycarbonate of Hexanediol. *International Journal of Adhesion and Adhesives* 31(8): 787–794. DOI: 10.1016/j.ijadhadh.2011.05.010

Glass, S. V, and Zelinka, S. L. 2010. Moisture Relations and Physical Properties of Wood. Forest Product Laboratory, Madison 1–20.

Gülzow, A., Richter, K., and Steiger, R. 2011. Influence of Wood Moisture Content on Bending and Shear Stiffness of Cross Laminated Timber Panels. *European Journal of Wood and Wood Products* 69(2): 193–197. DOI: 10.1007/s00107-010-0416-z

Gurunathan, T., Mohanty, S., and Nayak, S. K. 2015. Isocyanate Terminated Castor Oil-Based Polyurethane Prepolymer: Synthesis and Characterization. *Progress in Organic Coatings* 80: 39–48. DOI: 10.1016/j.porgcoat.2014.11.017

Hadjib, N., Massijaya, M. Y., and Hadi, Y. S. 2010. Address Technical Gaps in Producing Bio-Composite Products, Identify Suitable Wood Species and Evaluate Mechanical Properties. *Paper presented on Project Workshop CFC/ITTO: Utilization of Small Diameter Logs from Sustainable Source for Bio-Composite Products*. Institut Pertanian Bogor. Bogor.

Hariz, T. M. R., Hadi, Y. S., Lubis, M. A. R., Maulana, M. I., Sari, R. K., and Hidayat, W. 2023. Physical and Mechanical Properties of Cross-Laminated Timber Made of a Combination of Mangium-Puspa Wood and Polyurethane Adhesive. *Jurnal Sylva Lestari* 11(1): 37–65. DOI: 10.23960/jsl.v11i1.645

Hass, P., Wittel, F. K., Mendoza, Herrmann, H. J., and Niemz, P. 2012. Adhesive Penetration in Beech Wood: Experiments. *Wood Science and Technology* 46: 243-256. DOI: 10.1007/s00226-011-0410-6

Hazmi, A. S. A., Aung, M. M., Abdullah, L. C., Salleh, M. Z., and Mahmood, M. H. 2013. Producing Jatropha Oil-Based Polyol Via Epoxidation and Ring Opening. *Industrial Crops and Products* 50: 563–567. DOI: 10.1016/j.indcrop.2013.08.003

Hematabadi, H., Madhoushi, M., Khazaeian, A., and Ebrahimi, G. 2021. Structural Performance of Hybrid Poplar-Beech Cross-Laminated-Timber (CLT). *Journal of Building Engineering* 44: 102959. DOI: 10.1016/j.jobe.2021.102959

Hindman, D. P., and Bouldin, J. C. 2015. Mechanical Properties of Southern Pine Cross-Laminated Timber. *Journal of Materials in Civil Engineering* 27(9). DOI: 10.1061/(asce)mt.1943-5533.0001203

Hong, S., Gu, Z., Chen, L., Zhu, P., and Lian, H. 2018. Synthesis of Phenol Formaldehyde (PF) Resin for Fast Manufacturing Laminated Veneer Lumber (LVL). *Holzforschung* 72(9): 745–752. DOI: 10.1515/hf-2017-0184

Hovanec, D. 2015. Effect of Wood Characteristics on Adhesive Bond Quality of Yellow-Poplar for Use in Cross-Laminated Timbers. 99.

International Organization for Standardization (ISO). 1997. *Geometrical Product Specifications (GPS) Surface Texture: Profile Method. Terms, Definitions and Surface Texture*

Parameters. ISO 4287-1977. International Organization for Standardization. Geneva (SW).

Jankowska, A., Boruszewski, P., Drozdzek, M., Rębkowski, B., Kaczmarczyk, A., and Skowrońska, A. 2018. The Role of Extractives and Wood Anatomy in the Wettability and free Surface Energy of Hardwoods. *BioResources* 13(2): 3082–3097. DOI: 10.15376/biores.13.2.3082-3097

Japanese Agricultural Standard (JAS). 2019. *JAS 3079: Cross Laminated Timber*. Tokyo: Ministry of Agriculture, Forestry, and Fisheries.

Karacebeyli, E., Douglas, B. 2013. CLT Handbook US Edition. FPInnovations. Canada (CA).

Kim, J., Jun, S., Laksnarain, R., and You, S. M. 2016. Effect of Surface Roughness on Pool Boiling Heat Transfer at a Heated Surface Having Moderate Wettability. *International Journal of Heat and Mass Transfer* 101: 992–1002. DOI: 10.1016/j.ijheatmasstransfer.2016.05.067

Knorz, M., Schmidt, M., Torno, S., and Van De Kuilen, J. W. 2014. Structural Bonding of Ash (*Fraxinus excelsior* L.): Resistance to Delamination and Performance in Shearing Tests. *European Journal of Wood and Wood Products* 72(3): 297–309. DOI: 10.1007/s00107-014-0778-8

Kong, X., Liu, G., and Curtis, J. M. 2011. Characterization of Canola Oil Based Polyurethane Wood Adhesives. *International Journal of Adhesion and Adhesives* 31(6): 559–564. DOI: 10.1016/j.ijadhadh.2011.05.004

Lai, Y., Qian, Y., Yang, D., Qiu, X., and Zhou, M. 2021. Preparation and Performance of Lignin-Based Waterborne Polyurethane Emulsion. *Industrial Crops and Products* 170: 113739. DOI: 10.1016/j.indcrop.2021.113739

Lei, H., and Frazier, C. E. 2015. A Dynamic Mechanical Analysis Method for Predicting the Curing Behavior of Phenol-Formaldehyde Resin Adhesive. *Journal of Adhesion Science and Technology* 29(10): 981–990. DOI: 10.1080/01694243.2015.1011735

Lepage, R. T. M. 2012. *Moisture Response of Wall Assemblies of Cross-Laminated Timber Construction in Cold Canadian Climates*. UWSpace. Ontario, Canada.

Li, M. 2017. Evaluating Rolling Shear Strength Properties of Cross-Laminated Timber by Short-Span Bending Tests and Modified Planar Shear Tests. *Journal of Wood Science* 63(4): 331–337. DOI: 10.1007/s10086-017-1631-6

Liao, Y., Tu, D., Zhou, J., Zhou, H., Yun, H., Gu, J., and Hu, C. 2017. Feasibility of Manufacturing Cross-Laminated Timber using Fast-Grown Small Diameter *Eucalyptus lumbers*. *Construction and Building Materials* 132: 508–515. DOI: 10.1016/j.conbuildmat.2016.12.027

Liu, Y., Liang, H. Q., Li, S., Liu, D., Long, Y. J., Liang, G. D., and Zhu, F. M. 2019. Preparation of Waterborne Polyurethane with High Solid Content and Elasticity. *Journal of Polymer Research* 26(6). DOI: 10.1007/s10965-019-1795-4

Lu, Z., Zhou, H., Liao, Y., and Hu, C. 2018. Effects of Surface Treatment and Adhesives on Bond Performance and Mechanical Properties of Cross-Laminated Timber (CLT) Made from Small Diameter Eucalyptus Timber. *Construction and Building Materials* 161: 9–15. DOI: 10.1016/j.conbuildmat.2017.11.027

Luedtke, J., Amen, C., van Ofen, A., and Lehringer, C. 2015. 1C-PUR-Bonded Hardwoods for Engineered Wood Products: Influence of Selected Processing Parameters. *European Journal of Wood and Wood Products* 73(2): 167–178. DOI: 10.1007/s00107-014-0875-8

Machado, J. S., Louzada, J. L., Santos, A. J. A., Nunes, L., Anjos, O., Rodrigues, J., Simões, R. M. S., and Pereira, H. 2014. Variation of Wood Density and Mechanical Properties of

Blackwood (*Acacia melanoxylon* R. Br.). *Materials and Design* 56: 975–980. DOI: 10.1016/j.matdes.2013.12.016

Mallo, M. F. L., and Espinoza, O. 2014. Outlook for CLT. *BioResources* 9(4): 7427–7443.

Mardikanto, T., Karlina, L., and Bahtiar, E. 2017. *Sifat Mekanis Kayu*. IPB Press. Bogor.

Marko, G., Bejo, L., and Takats, P. 2016. Cross-Laminated Timber Made of Hungarian Raw Materials. *IOP Conference Series: Materials Science and Engineering* 123: 012059. DOI: 10.1088/1757-899x/123/1/012059

Martawijaya, A., Kartasujana, I., Mandang, Y. ., Kadir, K., and Prawira, S. A. 1989. *Atlas Kayu Indonesia Jilid II*. Pusat Penelitian dan Pengembangan. Bogor.

Na, B., Pizzi, A., Delmotte, L., and Lu, X. 2005. One-Component Polyurethane Adhesives for Green Wood Gluing: Structure and Temperature-Dependent Creep. *Journal of Applied Polymer Science* 96(4): 1231–1243. DOI: 10.1002/app.21529

Oliviero, M., Stanzione, M., D'Auria, M., Sorrentino, L., Iannace, S., and Verdolotti, L. 2019. Vegetable Tannin as a Sustainable UV Stabilizer for Polyurethane Foams. *Polymers* 11(3): 1–16. DOI: 10.3390/polym11030480

Poh, A. K., Sin, L. C., Foon, C. S., and Hock, C. C. 2014. Polyurethane Wood Adhesive from Palm Oil-Based Polyester Polyol. *Journal of Adhesion Science and Technology* 28(11): 1020–1033. DOI: 10.1080/01694243.2014.883772

Pooryousefy, E., Xie, Q., Chen, Y., Wood, C. D., Saeedi, A., and Sari, A. 2021. pH Effect on Wettability of –NH+-Brine-Muscovite System: Implications for Low Salinity Effect in Sandstone Reservoirs. *Journal of Molecular Liquids* 325: 115049. DOI: 10.1016/j.molliq.2020.115049

Roffael, E. 2016. Significance of Wood Extractives for Wood Bonding. *Applied Microbiology and Biotechnology* 100(4): 1589–1596. DOI: 10.1007/s00253-015-7207-8

Sheshmani, S. 2013. Effects of Extractives on Some Properties of Bagasse/High Density Polypropylene Composite. *Carbohydrate Polymers* 94(1): 416–419. DOI: 10.1016/j.carbpol.2013.01.067

Sheshmani, S., Ashori, A., and Farhani, F. 2012. Effect of Extractives on the Performance Properties of Wood Flour- Polypropylene Composites. *Journal of Applied Polymer Science* 123: 1563–1567. DOI: 10.1002/app.34745

Shi, S. Q., and Gardner, D. J. 2001. Dynamic Adhesive Wettability of Wood. *Wood and Fiber Science* 33(1): 58–68.

Sikora, K. S., McPolin, D. O., and Harte, A. M. 2016. Shear Strength and Durability Testing of Adhesive Bonds in Cross-Laminated Timber. *Journal of Adhesion* 92(7–9): 758–777. DOI: 10.1080/00218464.2015.1094391

Srivaro, S., Pásztory, Z., Le Duong, H. A., Lim, H., Jantawee, S., and Tomad, J. 2021. Physical, Mechanical and Thermal Properties of Cross Laminated Timber Made with Coconut Wood. *European Journal of Wood and Wood Products* 79(6): 1519–1529. DOI: 10.1007/s00107-021-01741-y

Srivaro, S., Tomad, J., Shi, J., and Cai, J. 2020. Characterization of Coconut (*Cocos nucifera*) Trunk's Properties and Evaluation of Its Suitability to be Used as Raw Material for Cross Laminated Timber Production. *Construction and Building Materials* 254: 119291. DOI: 10.1016/j.conbuildmat.2020.119291

Sunija, A. J., Ilango, S. S., and Kumar, K. P. V. 2014. Synthesis and Characterization of Bio-Based Polyurethane from Benzoylated Cashewnut Husk Tannins. *Bulletin of Materials Science*

37(3): 735–741. DOI: 10.1007/s12034-014-0665-2

Szycher, M. 2013. *Szycher's Handbook of Polyurethanes*. CRC Press. New York.

Technical Association of the Pulp and Paper Industry. 1991. *TAPPI Test Methods*. TAPPI Press, Georgia (GA).

Thébault, M., Pizzi, A., Essawy, H. A., Barhoum, A., and Van Assche, G. 2015. Isocyanate Free Condensed Tannin-Based Polyurethanes. *European Polymer Journal* 67: 513–526. DOI: 10.1016/j.eurpolymj.2014.10.022

Thomson, T. 2004. *Polyurethanes as Specialty Chemicals*. CRC Press, Boca raton. DOI: 10.1201/9781420039665

UNECE/FAO. 2020. *Annual Market Review 2019-2020 - Forest Products*. *United Nations Publication*.

Wang, H., Lin, F., Qiu, P., and Liu, T. 2018. Effects of Extractives on Dimensional Stability, Dynamic Mechanical Properties, Creep, and Stress Relaxation of Rice Straw/High-Density Polyethylene Composites. *Polymers* 10(10). DOI: 10.3390/polym10101176

Wang, Z., Fu, H., Gong, M., Luo, J., Dong, W., Wang, T., and Chui, Y. H. 2017. Planar Shear and Bending Properties of Hybrid CLT Fabricated with Lumber and LVL. *Construction and Building Materials* 151: 172–177. DOI: 10.1016/j.conbuildmat.2017.04.205

Wiesner, F., Thomson, D., and Bisby, L. 2021. The Effect of Adhesive Type and Ply Number on the compressive Strength Retention of CLT at Elevated Temperatures. *Construction and Building Materials* 266: 121156. DOI: 10.1016/j.conbuildmat.2020.121156

Yuniarti, K., Santoso, A., and Pari, R. 2020. The Effect of Drying Temperatures and Tannin-Adhesive Types on Bending Properties and Shear Strength of Glued *Eucalyptus pellita* Board. *IOP Conference Series: Earth and Environmental Science* 460(1). DOI: 10.1088/1755-1315/460/1/012015

Yusof, N. M., Tahir, P. M., Lee, S. H., Khan, M. A., and James, R. M. S. 2019a. Mechanical and Physical Properties of Cross-Laminated Timber Made from *Acacia mangium* Wood as Function of Adhesive Types. *Journal of Wood Science* 65(1). DOI: 10.1186/s10086-019-1799-z

Yusof, N. M., Tahir, P. M., Roseley, A. S. M., Lee, S. H., Halip, J. A., James, R. M. S., and Ashaari, Z. 2019b. Bond Integrity of Cross Laminated Timber from *Acacia mangium* Wood as Affected by Adhesive Types, Pressing Pressures and Loading Direction. *International Journal of Adhesion and Adhesives* 94: 24–28. DOI: 10.1016/j.ijadhadh.2019.05.010

Yusoh, A. S., Md Tahir, P., Anwar Uyup, M. K., Lee, S. H., Husain, H., and Khaidzir, M. O. 2021. Effect of Wood Species, Clamping Pressure and Glue Spread Rate on the Bonding Properties Of Cross-Laminated Timber (CLT) Manufactured from Tropical Hardwoods. *Construction and Building Materials* 273: 121721. DOI: 10.1016/j.conbuildmat.2020.121721

Zhang, Y., Xia, Z., Huang, H., and Chen, H. 2009. A Degradation Study of Waterborne Polyurethane Based on TDI. *Polymer Testing* 28(3): 264–269. DOI: 10.1016/j.polymertesting.2008.12.011

Zhou, J., Chui, Y. H., Niederwestberg, J., and Gong, M. 2020. Effective Bending and Shear Stiffness of Cross-Laminated Timber by Modal Testing: Method Development and Application. *Composites Part B: Engineering* 198: 108225. DOI: 10.1016/j.compositesb.2020.108225